Applied Energy 305 (2022) 117909

Contents lists available at ScienceDirect

Applied Energy

journal homepage: www.elsevier.com/locate/apenergy

Variable cost evaluation of heating plants in district heating systems considering the temperature impact

Peter Lorenzen [a,b,*], Carlos Alvarez-Bel [b]

[a] Hamburg University of Applied Sciences, Competence Center for Renewable Energies and Energy Efficiency (CC4E), Am Schleusengraben 24, 21029 Hamburg, Germany
[b] Universitat Politècnica de València, Instituto Ingeniería Energètica, Camino de Vera S/N, 46022 Valencia, Spain

HIGHLIGHTS

- Comparable evaluation of variable costs for renewable heat production technologies.
- Cost evaluation considering both supply temperature and part load ratio.
- Application to exemplary solar-thermal, geothermal, and industrial surplus plants.
- Proposal for a new comprehensive district heating operation methodology.

GRAPHICAL ABSTRACT

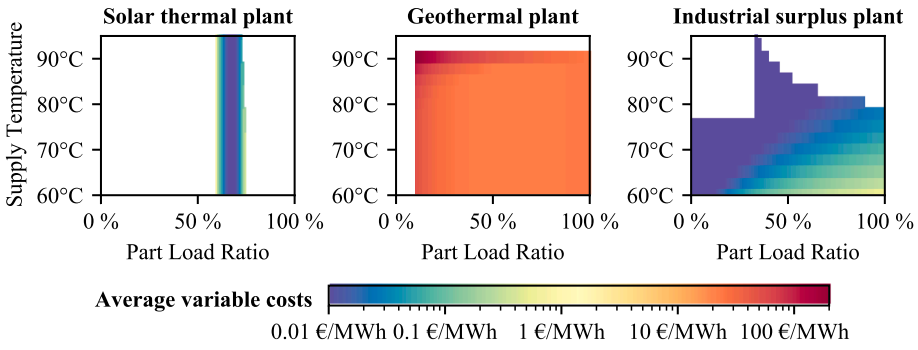

ARTICLE INFO

Keywords:
District heating systems
District heating transformation
Heating transition
Renewable heating plants
Heat production evaluation

ABSTRACT

District heating systems (DHSs) play an important role for urban areas as they enable an efficient and cost-effective heat supply. Existing DHSs are primarily based on fossil fuel energy and therefore need to be transformed in the coming years to meet the climate goals of the Paris Agreement. Lowering system temperatures is relevant to convert the fossil-based generation to renewable energy sources. However, there is a lack of a systemic methodology that can properly promote the required changes of the system temperatures during operation. This paper contributes a first part to such a methodology: a method to evaluate the average variable costs of heating plants that supply DHSs. The novelty of the approach lies in a systematic way to consider the impact of supply temperature and momentary thermal power on the variable costs of a plant. The method's requirements, application, results, and conclusions are demonstrated in three case studies of renewable heating plants: a solar thermal, a geothermal and an industrial surplus heating plant. The specific results of these case studies show that different set-points for the supply temperature and for thermal power of each plant have an impact on the variable cost of production. A comparison of the results demonstrates that the method increases the cost transparency in general. It is concluded that the supply temperature should be used as a variable in the operational optimization in DHSs. Further, the method should be part of a more comprehensive methodology for entire DHS infrastructures including storages, the network, and the customers.

* Corresponding author at: Hamburg University of Applied Sciences, Competence Center for Renewable Energies and Energy Efficiency (CC4E), Am Schleusengraben 24, 21029 Hamburg, Germany.
E-mail addresses: peter.lorenzen@haw-hamburg.de (P. Lorenzen), calvarez@die.upv.es (C. Alvarez-Bel).

https://doi.org/10.1016/j.apenergy.2021.117909
Received 10 May 2021; Received in revised form 1 July 2021; Accepted 17 September 2021
Available online 28 September 2021

Nomenclature

a_1	solar thermal first order loss coefficient, [–]
a_2	solar thermal second order loss coefficient, [–]
A_{coll}	collector surface, [m^2]
c_{av}	average variable costs, [€/MWh]
$c_{electricity}$	specific electricity costs, [€/MWh]
c_{others}	other specific costs, [€/MWh]
c_{fuel}	specific fuel costs, [€/MWh]
g	gravitational acceleration, [m/s^2]
G_t	total solar radiation, [W/m^2]
$P_{el,pump}$	pump's electrical power, [kW]
PI	geothermal productivity index, [$m^3/h/MPa$]
PLR	part load ratio, [–]
p_{WH}	well head pressure, [Pa]
$\dot{Q}$	thermal power, [MW]
$\dot{Q}_{coll}$	thermal power of solar thermal collector, [MW]
$\dot{Q}_{max}$	maximum thermal power, [MW]
$\dot{Q}_{min}$	minimum thermal power, [MW]
$r_{electricity}$	specific revenues for electricity production, [€/MWh]
T_a	ambient temperature, [K]
$\overline{T}_{coll}$	mean temperature of solar thermal collector, [K]
T_s	supply temperature, [K]
$T_{s,max}$	maximum supply temperature, [K]
$T_{s,min}$	minimum supply temperature, [K]
$\dot{V}$	volumetric flow rate, [m^3/h]
$\dot{V}_{nom}$	nominal volumetric flow rate, [m^3/h]
$\dot{V}_{pump}$	volumetric flow rate of the pump, [m^3/h]
z_{DFL}	dynamic fluid layer height, [m]
z_{SFL}	static fluid layer height, [m]

Greek symbols

Δp_{pump}	pump's pressure difference, [Pa]
Δp_{loss}	pressure loss, [Pa]
$\Delta\dot{Q}$	thermal power difference, [MW]
Δt	time difference, [s]
ΔT_s	supply temperature difference, [K]
η	efficiency, [–]
η_0	reference efficiency of solar thermal collector, [–]
η_{coll}	efficiency of solar thermal collector, [–]
η_{nom}	nominal pump efficiency, [–]
η_{pump}	pump efficiency, [–]
ρ	density, [kg/m^3]

Abbreviations

DH	district heating
DHS	district heating system
GHD	generation of district heating
KPI	key performance indicator
NGB	North German Basin (geological region)
PLR	part load ratio
SPECO	specific exergy costing
TES	thermal energy storage
3GDH	3rd generation of district heating
4GDH	4th generation of district heating
5GDH	5th generation of district heating

1. Introduction

The goal of the Paris Agreement is to limit global warming preferably to 1.5 °C by a drastic reduction of global greenhouse gas emissions [1]. The International Energy Agency reports that the heating sector contributed one half to the global final energy consumption in 2019 [2]. The share of renewable sources in the heating sector was estimated with 11 % and the still dominant fossil fuels emit 40 % of the global CO2 emissions. The United Nations Environmental Programme described district heating (DH) as "a best practice approach" for an efficient, affordable, and ecologic heat supply in urban areas [3]. But also, the supply for district heating systems (DHSs) must be transformed to renewable heat sources which have to be smoothly integrated into existing systems. Lund et al. define four generations of district heating (GDH) [4], whereas the 4th generation (4GDH) is based on renewable heat sources which require low system temperatures. In existing systems of older generations, barriers that come from technical restrictions [5] as well as economical lock-in effects caused by the low cost sensitivity for higher temperatures of the existing conventional technologies [6] hinder the lowering of the systems' temperatures.

The motivation for the paper arose from the synthesis of two aspects: First, the relevance of temperatures for district heating costs is known from long-term considerations (scenarios) [7] and second, a lack of systematic integration of the temperature quantity into the daily planning mechanisms of operation has been identified. Therefore, the overall goal is to transfer the findings from scenarios into a mechanism that independently optimizes the temperatures in operation. For this purpose, transparency of the temperature impact on the costs during operation is needed. A novel method for creating this transparency for the production side is presented in this paper.

The paper is organized as follows: The following chapter 2 reviews the existing practice in considering the supply temperature in the studies for DHS transformation as well as operation. Existing methods that include temperatures in economic DHS evaluations are presented. Even though several approaches exist, the lack of a methodological approach is identified. The review of existing concepts shows that they do not include the control of supply temperature and thermal power of the heating plants sufficiently in economic optimization and operational strategies. Particularly, there is no concept that includes the impact of these two quantities on average variable costs. A new method to fill this gap for the production side is proposed in chapter 3, which allows for comparing the temperature impact on average variable costs of different heating technologies. This method is applied to three relevant technologies for heating plants in future DHSs in chapter 4, using parameters from the existing Hamburg-Wilhelmsburg DHS (input parameters are given in the appendix A). The results for the individual plants are presented, compared with each other, and discussed in chapter 5 (further results are given in the appendix B). Finally, relevant conclusions, which emphasize the advantages of the proposed method and point out further required development for a comprehensive methodology, are stated in chapter 6.

2. Gap analysis

The following sections show the gap analysis related to the supply temperature impact in DHSs. To identify the methodological gap, three fields of current research are analyzed. The first section is focused on the impact of supply temperature and the identification of the optimal supply temperatures through scenario consideration. The second section covers the concept of dynamic supply temperatures in control strategies. The third section introduces concepts of including the dynamic temperature control in an economic optimization. Finally, a methodological gap in all three fields is identified.

2.1. Identifying the most economic temperature level of existing DHSs

The transformation from older GDH to 4GDH involves a broad field

of current research activities with a focus on "lower and more flexible temperature distributions" [8]. Transformation studies like [5] point out the challenges which require a whole system transition including temperatures, hydraulics, and operative procedures. The study developed key performance indicators (KPIs) to evaluate the whole transition progress including the temperature level. A common approach to evaluate the impact of temperatures on the transition process is the comparison of different scenarios with temperatures as constrains. As one example, Nord et al. have shown – by varying the supply temperature between 80 and 55 °C – that low supply temperatures are important to utilize renewable sources and that they are necessary for DHS in low heat density regions to increase the competitiveness to individual heating. Further they describe the trade-off between heat losses of the pipes at high supply temperatures and a higher electricity consumption at lower supply temperatures with higher flow rates [9].

Averfalk and Werner present an individual evaluation of different renewable heating technologies for two scenarios [6]. The first scenario uses the temperature levels of the 3rd GDH (3GDH) and the second one uses the lower 4GDH temperature levels. They include the internal temperature behavior of the plants, the heat losses in the system as well as peak-load production with biofuels to evaluate the impact from a system point of view. The electricity demand of pumps is neglected to simplify the evaluation. The central KPI is the cost reduction gradient given in (€/TJ/°C) which was introduced in [10]. Albeit providing a general evaluation of different technologies, the cost reduction gradient cannot be used as KPI for operational purposes like dynamic supply temperature control as presented in section 2.2, because it does not provide detailed information over the whole range of each control variable. Instead, this KPI allows for an aggregated evaluation of the impact of different temperature levels on costs at a system level to give design recommendations. The results of Averfalk and Werner show that heat losses do indeed play an important role, but lower production costs through a better utilization of non-combustion sources and consequently avoiding peak production are the most important factors for cost reduction in the transition from 3GDH to 4GDH. The overall result of their investigation is that (non-combustion) technologies based on renewable sources are much more sensitive to lower supply temperatures than the combustion-based technologies. Existing DHSs with a large share of these conventional technologies do not have high, direct economic incentives and therefore they form a barrier for the transition to lower temperatures which in turn results in a barrier for the integration of renewable sources.

The concept of the 5th GDH (5GDH) goes even further. Buffa et al. classify 5GDH as DHSs with supply temperatures below the required supply temperature. These systems use electricity (e.g. with heat pumps) at the substations to increase the temperature level for domestic hot water and space heating locally. In these systems, temperature, and thermal energy storages (TES) are controlled to minimize operational costs with special regard to electricity prices and thermal load prediction [11]. The supply temperature of heat sources in some of these systems can thus vary inside a considerable range [12].

To find the optimal supply temperature, Lund et al. present a long-term analysis of temperatures from a societal point of view to provide general recommendations [7]. The analysis is based on scenarios that consider different temperature regimes and calculate socioeconomic costs (including costs for emissions). The interim result of its evaluation shows that a temperature reduction down to 55 °C is beneficial. Further temperature reductions (5GDH) currently require high investments for the substations because heat pumps must be integrated.

In addition to the economic perspective, Rämä et al. showed that the share of renewable heat sources could be increased by lowering the temperatures [13].

2.2. Control strategies for supply temperature

The studies mentioned in section 2.1 show the relevance of detailed evaluation of DH temperatures. The optimal temperature depends strongly on the given DHS and a general statement cannot be made. Additionally, it is common practice in DHS to vary the supply temperature on longer timescales (e.g. seasonal) within small ranges. To increase the benefit of dynamic supply temperatures, new concepts based on non-uniform temperatures should be explored as described below.

One innovative concept is the non-uniform temperature district heating [14] where the temperature is not constant over the day. In short periods of the day, the system's temperature may be increased up to 75 °C and heat for domestic hot water is then stored in decentralized TESs. In other times, the temperature is lowered down to 40 °C to reduce heat losses in transmission. With decentralized heat pumps, temperatures may be reduced even further [15].

In the context of time-dynamic temperature variations, the thermo-mechanical impact on the pipes must be considered. Temperature variations cause thermomechanical stress in the pipes [16]. This stress causes damage which is accumulated over the lifetime and can be calculated by damage theories with some uncertainties induced by the different amplitudes that occur during operation: The higher the temperature amplitudes are, the more they reduce a pipe's lifetime. Further, the authors propose the introduction of an assessment strategy to allow for a better forecast of the ageing of pipes.

In contrast to a time-dynamic supply temperature, there can be locally heterogeneous temperatures. For example, it can be beneficial to combine different GDH e.g. by cascading one network to another [17].

Increasing the temperature leads to lower flow rates and therefore to lower electricity consumption for the grid pump but it increases the heat losses in the grid. With an increasing number of decentralized renewable heat sources, the degrees of freedom of a system increase, because every point of feed-in can have its own set-points for supply temperature and thermal power. Finding a cost minimum of such a system requires complex optimization strategies as presented in section 2.3.

2.3. Cost optimization including temperature control in DHS

Most modeling approaches for optimization do not embrace the system temperature as an optimization result. The review presented in [18] gives an overview over modelling and optimization approaches in DHSs. Instead of utilizing the supply temperature as a variable, the reviewed studies use different scenarios with constant input temperatures or the concept of exergy.

Exergy is a mature concept of combining energy and temperature in thermodynamics [19]. Based on this aggregated quantity, economic studies have been developed – so called exergo-economic analyses. One example is the specific exergy costing (SPECO) method [20]. The method analyzes all streams of exergy and their costs. It is suitable to identify technical enhancement potential (e.g. replacing ineffective heat exchangers) or operational optimization. The SPECO method has been applied to different types of DHSs e.g. with geothermal heat sources [21]. The exergy method can also be combined in multi-objective optimization approaches to allow for an evaluation of costs and exergy efficiency [22]. The advantage of this exergo-economic analysis is that aggregating temperature and energy to exergy simplifies the evaluation. A disadvantage is that through the aggregation, important information about the temperature is lost.

Because of the complexity of the required modelling, only a limited number of optimization studies exist that include supply temperatures. Pirouti et al. evaluated the supply temperature as an input variable in the analysis [23]. They included the pumping costs and the heat losses of the grid. One of their results is that a variable flow and supply temperature strategy benefits their considered cases. Vesterlund et al. optimized the pumping power and supply temperature in a system with multiple heat sources and came to the result that the temperature should be as low as possible [24]. Bavière et al. demonstrated their operational concept based on a model-predictive controller showing the benefits of variable supply temperatures in case of decentralized feed-in [25]. Fang et al. used genetic

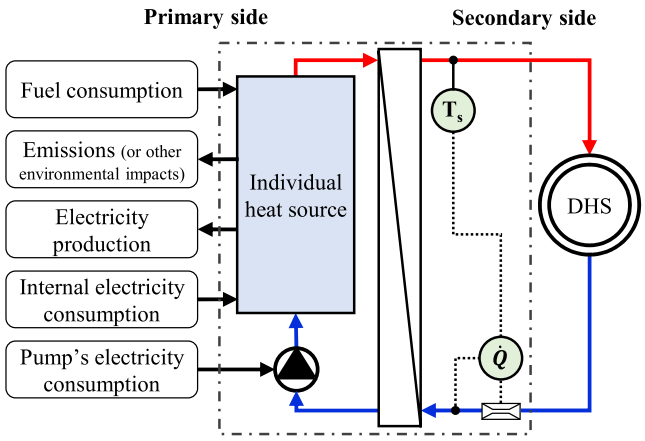

Fig. 1. Boundary conditions for each individual heating plant.

algorithms including costs for fuel, pumping power and losses [26]. The fuel consumption was assumed to be linear to the heat production. They found that the optimum between pumping costs and supply temperatures varies with the network characteristics. All these studies optimized the pump energy against the heat losses in the grid, but none of them included the impact of supply temperature on generation costs.

Another way to promote economically efficient operation is the use of innovative market mechanisms, such as the smart market concept. A smart market uses a mechanism based on computations which include the allocation of the products in the price clearing mechanism while eventually including transport costs [27]. The smart market in the sense of an allocating auction mechanism is not to be confused with the definition in [28] for "smart energy markets" that is focused on the interdependencies of different energy sectors markets. The concept of smart markets has been investigated for electricity grids [29] and gas grids [30] as well as for other network structures like communication networks [31] and water systems [32]. In literature, it could not be found that such a smart market has been developed for the district heating sector yet, but the idea of introducing smart market algorithms including a price for temperatures has been proposed in [33]. An advantage of the market mechanism is that they can be used for DHSs which are organized either in a strict vertically integrated form or in more competitive forms.

2.4. The gap in existing approaches

Temperatures have an impact on variable heat production costs. An example for this are geothermal heat sources with low reservoir temperatures which therefore require heat pumps to achieve a certain supply temperature level [7]. The lower the DHS supply temperature is, the lower are the electricity demand of the heat pump and thus the variable costs. Another impact is on maximum production, e.g. in solar thermal collectors. Their efficiency decreases with increasing supply temperature resulting in a lower thermal power [34]. These effects can be included in scenario evaluations which vary the temperature levels and thereby can give specific recommendations for the overall DHS design. But as scenario evaluations do not provide detailed information correlated to the whole range of each controllable variable, they do not satisfy the requirements for the daily operation. Further, even though numerous approaches of DHS evaluation and optimization exist, a comprehensive approach considering all degrees of freedom (in temperature and thermal power control) as variables in optimization and operational strategies is missing. This is identified as methodological gap which results from necessary simplifications to reduce the considerable operative complexity of controlling both dynamic supply temperature and thermal power control of distributed heat sources.

This paper addresses the methodological gap by creating a direct correlation between temperatures, thermal power, and average variable costs. The meta concept of opportunistic coordination is used to be able to handle the resulting complex techno-economical systems. It is based on the principle of opportunism and the principle of least commitment [35]. According to the opportunism principle, all degrees of freedom of a system must be considered. The principle of least commitment means that decisions should be taken as late as possible. Consequently, temperatures should be considered as both variables and outputs of the economic evaluation. Applying this meta concept means that all locations in DHSs must be considered for control where the temperature or the thermal power can be adjusted. To support the control decisions, the impact on costs at each controllable point must be known in correlation to the control variables. The locations can be found at pumps, valves, and heat exchangers. To facilitate such a smart system, a comprehensive and systemic methodology must be developed for all levels of the DHS including the heating plants, TESs, the piping network, the substations, and the customers' heating systems. Such a methodology can be key for low and dynamic temperature applications like grid cascades, decentralized feed-in and non-uniform (in time and location) temperature operation.

To contribute a first part to the future methodology, the objective of this paper is to support the principle of opportunism by increasing the transparency of variable costs correlated to the supply temperature as well as thermal power in steady-state production processes. To do so, a new method for the average variable cost evaluation was developed. The resulting average variable costs can be utilized to combine heating plants with different supply temperatures at the same location to deliver a minimum required supply temperature at cost-optimal points of operation from a system perspective. For the demand side, the increased transparency of the temperature impact on costs can be used to support demand side measures like demand side management or efficiency enhancement. Finally, the results should be embedded in an overall system optimization (e.g. in form of a smart market) that considers the flexibility of TESs, the customers, and the network operation.

3. General method for average variable cost evaluation of heating technologies including supply temperature and part load ratio

The method is innovative by correlating the average variable costs for heat production with the thermal power and supply temperature which are given in form of a discrete pattern. The objective is the development of a general method for the production side in DHSs that fits into an overall approach as described in section 2.4 and can be applied to all types of plants with a two-pipe connection. To achieve comparable results, the following preconditions are considered:

The objective is the evaluation of variable costs in the scope of operational system optimization. Therefore, fixed costs that occur e.g. from investments or staff salaries are not considered. For heat sources that are owned by third parties (e.g. in case of industrial surplus heat), additional variable costs can arise from the tariffs that are arranged in the contracts between the DH and the heat supplying companies. The supplying companies need these revenues to finance their investments (e.g. for assets for the heat extraction from industrial processes) or to be incented for the production in general. Such costs are neglected, because firstly, the origins are fixed costs and secondly, there are no standard tariffs that can be applied for this type of contracts. Further, the economic benefit of substituting other heating technologies (opportunity cost) will not be included in the evaluation of an individual heating plant. Instead, the presented method should be applied to all existing heating plants in the evaluated system including fossil or peak-load production to create a comparable data basis for a subsequent optimization.

The basic concept of the method is presented in Fig. 1 which shows the thermodynamic system boundary (dash-dotted line). All internal costs and conditions that emerge inside the system as well as external costs and conditions that act on the system must be identified. Therefore, the method requires the knowledge of the physical principle of each technology and the different impacts of the thermal and hydraulic

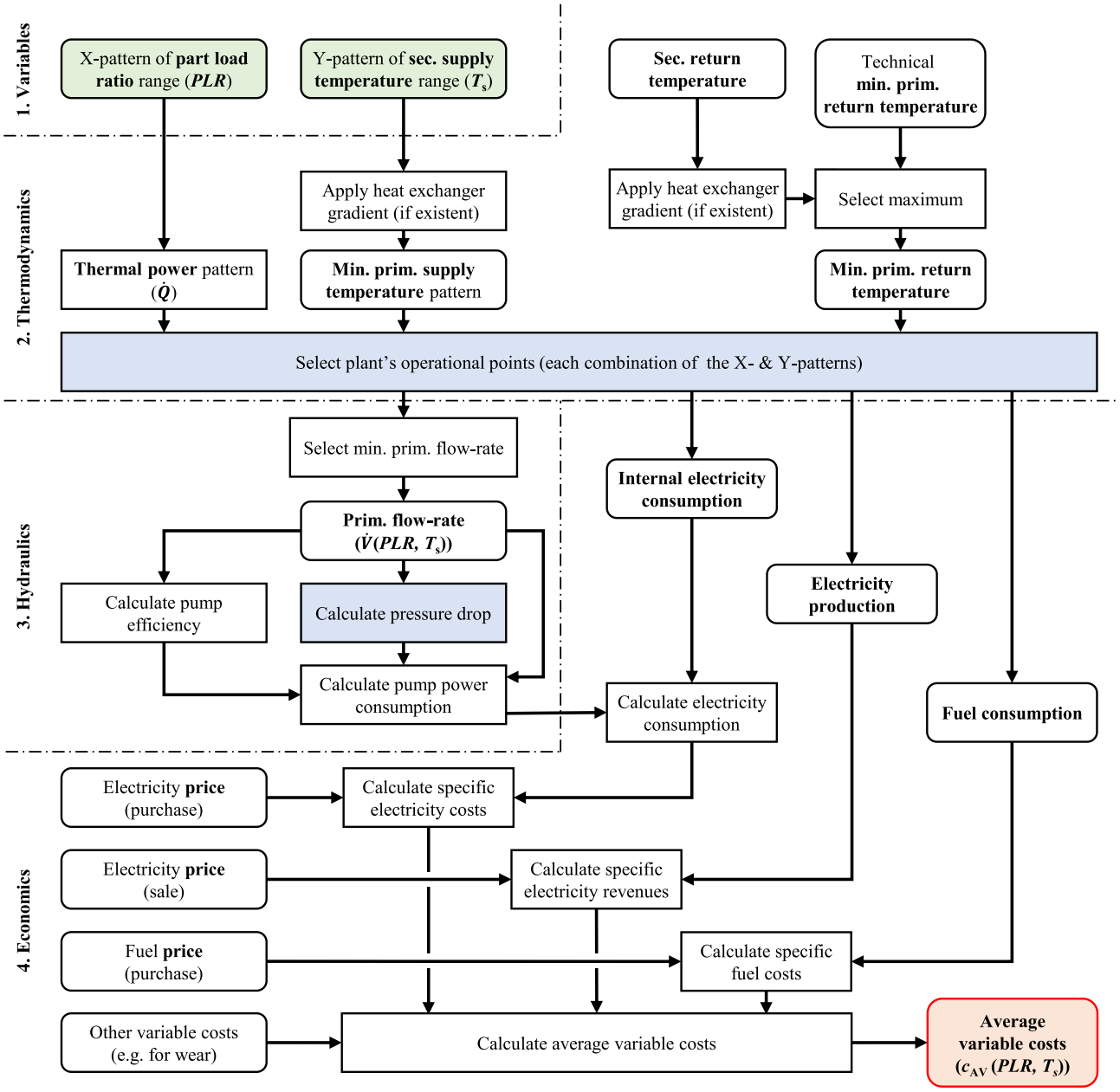

Fig. 2. Method for average variable cost calculation correlated to supply temperature and thermal power.

characteristics on variable costs. Fig. 1 presents the boundary conditions of any abstract heating technology (highlighted blue) as well as the measurements of two variables on the secondary side (highlighted green). In the presented case, a heat exchanger is included to separate the different hydraulic circuits and to control the secondary side supply temperature. While not all heating plants require this separation, control over the supply temperature can be achieved with other components such as mixing valves. These different variants of heating plant integrations as well as the specific hydraulic circuit designs (e.g. valves and TES) on the secondary side require an additional evaluation for the electricity demand of the secondary pump on an energy central level. However, heating plants with same size and secondary side integration will have the same electricity demand behavior on the secondary side correlated to different secondary supply temperatures. Therefore, the electricity demand of the secondary side is not included in this evaluation. In contrast to the secondary supply temperature, the secondary return temperature is an external condition that cannot be controlled from the production side.

The variable costs mainly occur as a result and balance of energy production and consumption as well as from other minor factors such as wear. As shown in Fig. 1, energy costs can come from fuel consumption (e.g. in boilers), electricity production (e.g. in combined heat and power plants), internal electricity consumption (e.g. in heat pumps) and the electricity consumption of one or more primary pumps. In some cases, additional costs can occur from penalties for environmental impact like emissions (e.g. CO2 taxes). If these costs must be considered, they are mostly internalized in the fuel or electricity costs. Therefore, they will not be mentioned separately in the method.

The method is based on a discrete, numerical concept for steady-state points of operation and requires discrete patterns of supply temperature and part load ratio (PLR) which additionally allow for a good comparability of different types of heat generation technologies. The numerical concept has several advantages. It allows for using non-linear equations and thus it does not require simplification in terms of linearization in the numerical heating plant model. Further, it allows for using data-driven models based on measurement data as an alternative to models based on

theoretical calculations. The steady-state concept simplifies the evaluation by excluding the time dimension (which could be considered by further developments of the method). Consequently, the analyzed operational period (Δt) can be chosen freely (e.g. 15 Minutes or 1 h).

The calculations are implemented in the Python programming language together with the packages NumPy [36] and Pandas [37]. Pandas is used to organize the results in a table called "data frame" provided by the package [38]. Fig. 2 shows the different steps of the evaluation. The two main variables (1) are used as inputs for the thermodynamic calculations (2). Based on the results, the hydraulic calculations can be done (3). The technical results from thermodynamics and hydraulics are then used to calculate the average variable costs (4). All details are explained in the following sections 3.1–3.4.

3.1. Variables of the evaluation

The usage of the PLR, a relative quantity that expresses a current thermal power output (highlighted green), allows for a comparability of plants with different maximum thermal power. The PLR is the quotient of current thermal power ($\dot{Q}$) and maximum power ($\dot{Q}_{max}$) (equation (1)).

$$PLR = \frac{\dot{Q}}{\dot{Q}_{max}} \tag{1}$$

The discrete PLR is defined by equation (2), and it depends on the resolution of the chosen step width ($\Delta\dot{Q}$) and the minimum thermal power ($\dot{Q}_{min}$). The minimum thermal power is defined as the smallest thermal power that is allowed during operation.

$$PLR = \frac{y\cdot\left(\dot{Q}_{min} + x\cdot\Delta\dot{Q}\right)}{\dot{Q}_{max}}, \quad \text{for} \quad y \in \{0,1\},$$

$$x \in N \wedge 0 \le x \le \frac{\left(\dot{Q}_{max} - \dot{Q}_{min}\right)}{\Delta\dot{Q}} \tag{2}$$

The secondary supply temperature (T_s, highlighted green) is defined by equation (3). Its step size—the temperature difference (ΔT_s)—is chosen with 2.5 K. Indeed, a higher resolution would be more precise but in practice, due to temperature controllers' inaccuracies, set-values beyond such precision could never be achieved in real operation.

$$T_s = T_{s,min} + x\cdot\Delta T_s,$$

$$\text{for} \quad x \in N \wedge 0 \le x \le \frac{T_{s,max} - T_{s,min}}{\Delta T_s} \tag{3}$$

3.2. Thermodynamic calculation

Lowering the return temperature would have a strong impact on the variable costs [39] and is objective of many studies. However, for the sake of simplicity and because of the focus to supply temperature, a constant secondary return temperature is assumed for this evaluation. However, there would be no problem to relax this restriction and include it as an additional variable. The minimum values of primary supply and return temperature can be calculated by applying the temperature gradient of the heat exchanger to the secondary temperatures. In most cases, the primary return temperature should be controlled to be as low as possible. But in some cases, it can be increased to control the thermal power or must be increased due to specific technical constrains.

The next step is the vital part of the calculations (large blue box in Fig. 2). It must be implemented individually for each technology and examples are presented in the following case studies. The internal set-points for each combination of PLR and supply temperature are chosen, if the combination is possible within the technical constrains. Each possible set-point combination represents a row in the results table. The first columns include the combinations of PLRs (X-dimension) and supply temperatures (Y-dimension). The following columns include the internal electricity consumption (e.g. for heat pumps), fuel consumption (e.g. for boilers) as well as electricity production (e.g. for combined heat and power plants). Another column includes the primary flow rate ($\dot{V}$) on the primary side which is used for the following hydraulic calculations.

3.3. Hydraulic calculation

The primary flow rate causes a pressure drop (Δp_{pump}) which must be calculated individually for each plant (small blue box in Fig. 2). The pressure drop and the flow rate ($\dot{V}_{pump}$) combined with the pump's efficiency (η_{pump}) allow for calculating the pump's electrical energy consumption ($P_{el,pump}$), which is also included in a separate column in the results table.

$$P_{el,pump} = \dot{V}_{pump}\cdot\Delta p_{pump}\cdot\frac{1}{\eta_{pump}} \tag{4}$$

3.4. Economic calculation

The primary side pump's electricity demand and the internal electricity demand can be summarized to calculate the specific costs for electricity consumption ($c_{electricity}$). The same can be done for the fuel consumption (c_{fuel}). Electricity production (e.g. via combined heat and power plants) results in specific revenues ($r_{electricity}$) which reduce the variable costs. Together with other specific costs (c_{others}) that are related to the duration of operation (e.g. costs for wear), these lead to the variable costs (c_{AV}) (red box in Fig. 2) as shown by equation (5). All costs are included as separated columns in the results table.

$$c_{AV}(PLR, T_s) = c_{electricity}(PLR, T_s) - r_{electricity}(PLR, T_s) + c_{fuel}(PLR, T_s) + c_{others} \tag{5}$$

3.5. Presentation of results

The results of the evaluation are three-dimensional and therefore an intuitive presentation is challenging. For quantitative utilization, important results will be given as tables in the appendix. A graphical representation should be used to express the correlation in a qualitative way and to compare magnitudes of costs. The visualization according to the described rules is an essential part of the new method and can be reproduced for future applications of the method. For figures presented in the following, a colored mesh plot from the package Matplotlib [40] is used. The plot axes represent the PLR and supply temperature ranges and are uniformly limited to achieve comparability of the plots. The average variable costs are colored in the colormap "spectral" in logarithmic and uniform scale. Costs that are below 0.01 €/MWh are rounded up and costs over 200 €/MWh are rounded down. The uniformity and the logarithmic scale allow for comparing the different plants even though their cost results ranges may differ considerably.

4. Case studies and specific implementation

The developed method is demonstrated by its application to selected plants. As this development is part of the research project Smart Heat Grid Hamburg, the case studies are defined according to plants of the DHS in Hamburg-Wilhelmsburg [41], which can be classified as 3GDH in the transition towards 4GDH. The cases include an existing solar thermal plant (700 kW), a planned geothermal plant (9300 kW) and an existing industrial surplus heating plant (300 kW). The individual implementations of the models will be presented in the following sections 4.1–4.3.

The most important hydraulic (e.g. pressure drop for pump energy consumption) and thermal conditions (temperatures and enthalpy flows) are implemented in a simplified way to demonstrate the method.

Table 1
Global parameters for all case studies.

Quantity	Value	Reference
Specific heat capacity (all circuits, except geothermal medium)	4.192 kJ/(kg K)	[45]
Density (all circuits, except geothermal medium)	976 kg/m^3	[45]
Secondary return temperature	50 °C	[41]
Max. secondary supply temperature	95 °C	[41]
Heat exchanger gradient	3 K	Assumption.
Taxes and levies (<100 MWh)	122 €/MWh	Sum of several elements from [46,47,48,49].
Taxes and levies (>100 MWh)	99.2 €/MWh	Sum of several elements from [46,47,48,49].
Grid fee (low voltage)	38.6 €/MWh	[50]
Grid fee (high voltage)	16.6 €/MWh	[50]
Electricity costs (incl. 20 % procurement)	44 €/MWh	[51]; volume weighted mean day ahead electricity price in 2019.

These general simplifications are described in the following.

The hydraulic calculation considers pressure losses of pipes using the methods from [42] and equations from [43] as well as pressure losses caused by heat exchangers simplified by quadratic regression. Other pressure losses are analyzed individually per technology. The efficiency of the pumps (η_{pump}) is simplified by equation (6), cf. [44]. It depends on the volumetric flow rate ($\dot{V}_{pump}$) as well as on the nominal pump values for volume flow rate ($\dot{V}_{nom}$), and efficiency (η_{nom}).

$$\eta_{pump} \approx 1 - (1 - \eta_{nom}) \cdot \left(\dot{V}_{nom} / \dot{V}_{pump} \right)^{0.1} \tag{6}$$

Thermodynamic equations are needed to consider the supply temperature as well as to calculate the required flow rates. These equations must be implemented individually for each heat source and they are presented in the respective subsection. Heat exchangers are included in a simplified way by assuming a fixed temperature gradient. The required plant parameters are basically taken from publicly available references or they are estimated. The global parameters are presented in Table 1.

4.1. Case 1: Solar thermal heating plant

The first case is the existing solar thermal plant on top of the "Energiebunker" in Hamburg-Wilhelmsburg [52], where evacuated tube collectors are used in two sizes: "Ritter XL 34P" and "Ritter XL 50P". Each of the 63 parallel collector rows installed consists of two "XL 34P" and three "XL 50P" [53] modules. The plant has a maximum thermal power of approximately 700 kW.

The costs of operation are evaluated by considering the electricity consumption of the pumps to overcome the pressure losses that are caused inside collectors, pipes, and the heat exchanger. The pressure drop of the collector is determined by quadratic regression using data from [54]. All component dimensions (e.g. pipe diameters) are determined by a design calculation based on local weather conditions as well as critical hydraulic conditions. The plant's parameters are shown in Table A1.

The collector's heat production ($\dot{Q}_{coll}$) can be calculated using equation (7) with the collector surface (A_{coll}), collector efficiency (η_{coll}) and total solar irradiance (G_t) [34]. The expression for solar thermal collector efficiency is standardized by [55] in equation (8). The efficiency correlates with the mean collector temperature ($\overline{T}_{coll}$), the ambient temperature (T_a) and the total solar irradiance. The zero-loss efficiency (η_0) as well as first and second order loss coefficient (a_1, a_2) are parameters given by manufacturers [56]. The mean collector temperature is the average of the collector's supply and return temperature [34].

$$\dot{Q}_{coll} = \eta_{coll} \cdot A_{coll} \cdot G_t \tag{7}$$

$$\eta_{coll} = \eta_0 - a_1 \cdot \frac{\overline{T}_{coll} - T_a}{G_t} - a_2 \cdot \frac{\left(\overline{T}_{coll} - T_a \right)^2}{G_t} \tag{8}$$

Equations (7) and (8) show the high impact of ambient temperature and solar irradiance on the thermal production. Consequently, different weather conditions must be evaluated separately which can be done by using weather forecast data. For this case study, an exemplary solar irradiance of 700 W/m^2 and ambient temperature of 18 °C will be assumed.

4.2. Case 2: Geothermal heating plant

The geothermal heating case study analyzes a deep hydrothermal doublet that is planned for the DHS in Hamburg-Wilhelmsburg with a depth of approximately 3500 m [57]. As this plant is currently in the planning phase, there is no public data available. Therefore, a hypothetical example is created which is based on parameters and assumptions from literature. Most parameters refer to a literature reference case ("heating plant 1" in [58]) which has a depth of 3000 m. The relevant components of the plant are an extraction well with a down-hole pump, the closed heating system at the surface including a heat exchanger and other periphery as well as an injection well. In the underground, the system is hydraulically open and the geothermal medium flows between the outlet of the injection well and the inlet of the extraction well. Detailed parameters for the components and the geological composition are listed in Table A2.

The maximum primary supply temperature equals the geothermal extraction temperature. The extraction temperature itself depends on the geological characteristics and the wells. Particularly relevant for the presented evaluation are the temperature in the considered depth (reservoir temperature) as well as the heat losses in the well.

The reservoir temperature of different wells can differ on a large scale, due to different local geological conditions [58]. Hamburg lies in a geological region called "North German Basin" (NGB). The local geological conditions effect the extraction temperature which can vary in a broad range and can only be verified after a well has been drilled. For the projected plant it is estimated with 130 °C by the executing company [57]. Because of the uncertainty, different values for the reservoir temperature have been considered in an upstream sensitivity analysis applied to the evaluation method. The here presented case assumes a relatively low reservoir temperature of 97 °C. However, although the chosen temperature is low, the variant is of realistic magnitude since an existing plant in Neustadt-Glewe has an extraction temperature of 97 °C at a depth of 2450 m and it is also located in the NGB [59].

The temperature reduction in the well is computed in correlation to the flow rate. To do so, it is assumed that the underground temperature increases linearly from 8 °C [60] near the surface to 97 °C at the bottom. The well is divided into 1 m long cylindric elements. Each element's temperature results from the heat transfer from the inner medium to the underground and is calculated using parameters (Table A2) and equations from [61]. The calculation has been verified by the data given in [60].

The minimum injection temperature is assumed to be 60 °C to prevent precipitation [58]. This data set results in a maximum thermal power of 9.3 MW.

The relevant parts for the hydraulic calculation of this plant are the wells including the down-hole pump as well as the heat exchanger on the surface. The pressure difference of the hydraulic open system is calculated by equation (9) from [58] to determine the electricity demand of

Table 2
Reference studies of other geothermal reservoirs.

Site	Max. flow rate	Productivity index	El. power	Reference
Case study, Hamburg, Germany (NGB)	70 l/s	30 m^3/h/MPa	1150 kW	
Textbook example	77 l/s	30 m^3/h/MPa	1270 kW	[58]
Bavaria, Germany	145 l/s	290 m^3/h/MPa	1050 kW	[62]
Alasehir, Turkey	69 l/s	745 m^3/h/MPa	157 kW	[61]
Kizildere, Turkey	63 l/s	–	250 kW	[63]
Groß Schönebeck, Germany (NGB)	–	0.6..15 m^3/h/MPa	–	[64]
West Mecklenburg-Vorpommern, Germany (NGB)	–	22..40 m^3/h/MPa	–	[65]

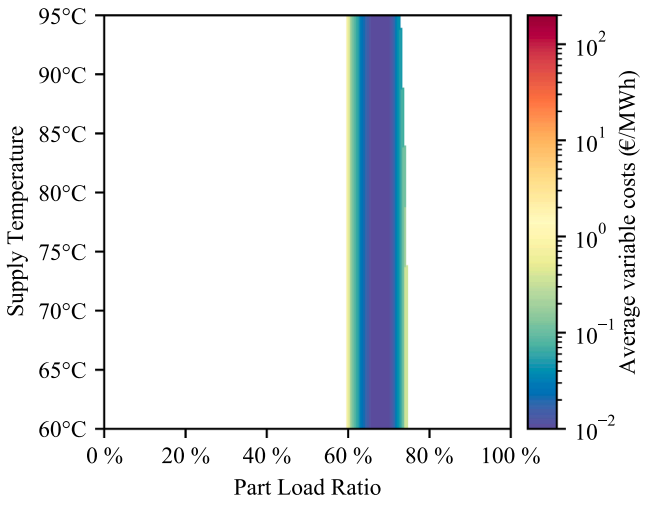

Fig. 3. Average variable costs of the solar thermal plant at 700 W/m^2 and 18 °C.

Table 3
Extraction temperature depending on flow rate for the geothermal plant.

Flow rate (l/s)	10	20	30	40	50	60	70
Extraction temperature (°C)	75.7	85.1	88.7	90.5	91.7	92.5	93.0

the downhole pump.

$$\Delta p_{\text{pump}} = p_{\text{WH}} + \Delta p_{\text{loss}} - \rho \cdot g \cdot z_{\text{DFL}} \tag{9}$$

The term consists of three parts: the static wellhead pressure (p_{WH}) to prevent degassing in the geothermal-medium, the friction of the well pipes (Δp_{loss}), which can be calculated from the pipe's characteristics, and the pressure resulting from the dynamic fluid level height (z_{DFL}). The dynamic fluid level can be calculated by equation (10) [58] and is responsible for the main pressure loss. It describes the fluid level in the ground that is reduced by the pump from the static fluid level (z_{SFL}) to the dynamic fluid level. The geothermal productivity index (*PI*) represents the characteristics of the geological formation.

$$z_{\text{DFL}} = z_{\text{SFL}} + \frac{\dot{V}}{PI \cdot \rho \cdot g} \tag{10}$$

Applying the equations to the parameters which are given in the appendix (Table A2) results in a maximum electrical consumption of the geothermal pump of 1150 kW for this case. To verify the magnitude of the electricity consumption, the pumping power is compared to different reference cases in Table 2. Due to the different productivity indices as well as other different parameters, which are related to the individual

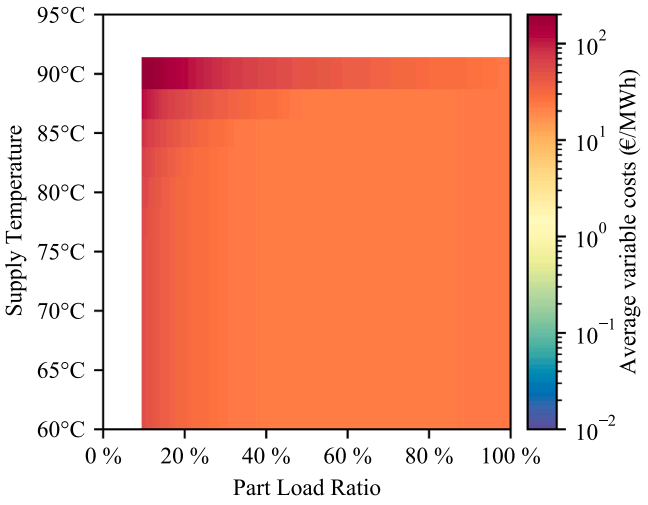

Fig. 4. Average variable costs of the geothermal plant.

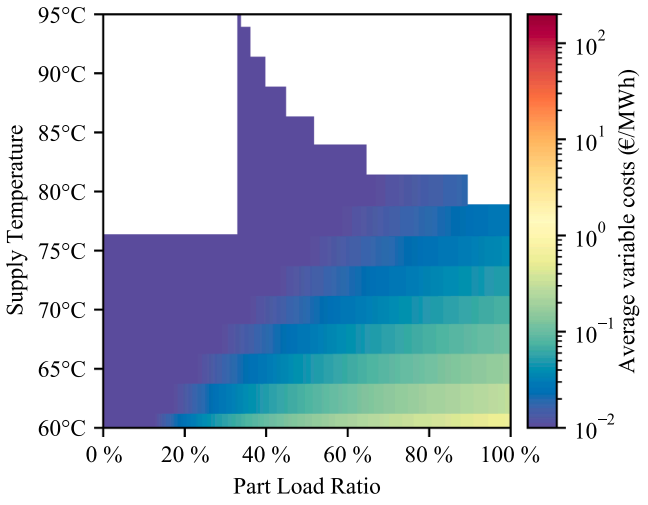

Fig. 5. Average variable costs of the industrial surplus heating plant.

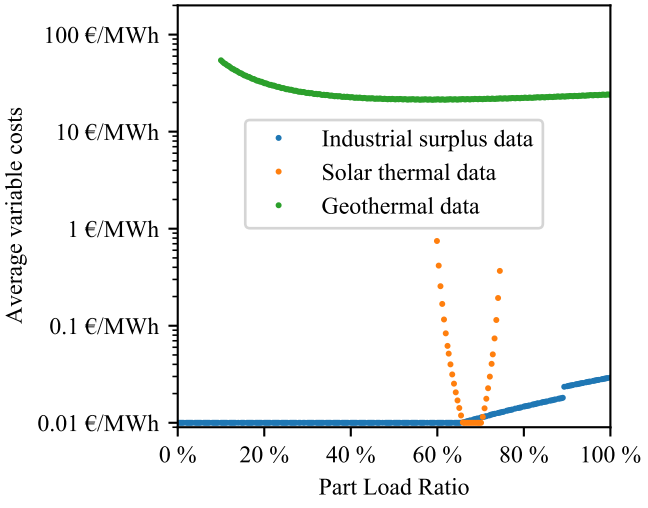

Fig. 6. Minimum average variable costs over PLR of all case studies.

geological regions, the shown case studies are hardly comparable. However, the magnitude of the electrical pumping power is plausible, but the relatively low productivity index results in a high demand for electrical power. It can also be taken from the table that studies investigating the same geological region (NGB) indicate a plausible

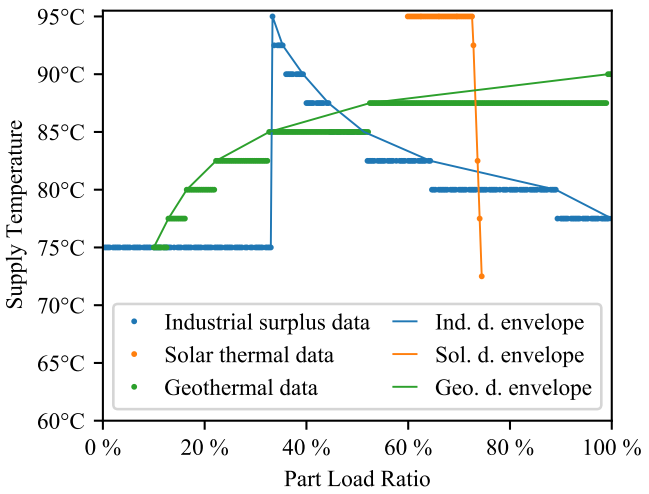

Fig. 7. Maximum temperature at minimum average variable costs over PLR for all case studies – data points from evaluation and envelope curves for each heating plant.

magnitude for the assumed productivity index. Due to the lack of availability of other data, the chosen geothermal productivity index of 30 m^3/h/MPa is acceptable. The impact of the uncertainty on the quantitative validity of these assumptions will be discussed in section 5.4.

The main costs occur from the electricity consumption of the down-hole pump. In addition to the electricity consumption, costs occur from worn parts and components due to the high mechanical stress of the down-hole pump. These are estimated with 40 € per hour of operation. More economic details and parameters can be found in Table A3.

4.3. Case 3: Industrial surplus heating plant

Industrial surplus heating plants reuse heat that is a byproduct of an industrial process and would otherwise be emitted to the environment [66]. The potential and efficiency of industrial surplus heat is strongly related to the temperature level of the surplus heat source as well as demand side temperatures [67]. The characteristics of these types of heating plants depend strongly on the local heat sources and their hydraulic integration.

The case of interest here is a surplus heat plant that is in operation in Hamburg-Wilhelmsburg [68]. The plant can be simplified to two types of processes. The first process (A) uses exhaust gas heat, can produce 100 kW at a maximum temperature of 95 °C and if enabled, it can only run at full thermal power. The second one (B) is a cooling process with 200 kW and a maximum temperature of 75 °C. Using a downstream cooling tower, the amount of heat led off can be adjusted. The plant's supply temperature is the mixing temperature of both streams. The electrical energy consumption depends on the pressure losses of the process heat exchangers and the pipes to overcome the distance on the industrial site (300 m). More parameters are listed in Table A4.

5. Results and discussion

The results of the case studies are described in the following sections. In the first three sections, the individual result of each case is presented by the previously introduced plot and its data is interpreted. The case studies are then compared, discussed and general conclusions are derived.

5.1. Case 1: Results for solar-thermal heating

The resulting average variable costs for the solar thermal plant are presented in Fig. 3. Because of low pressure loss inside the system and resulting low power consumption for the pump, the average variable costs are low. The high efficiency of the evacuated tube collectors leads to a high possible supply temperature and a small control range of the PLR. The supply temperature is almost independent from the chosen PLR. Only for maximum PLR, the full supply temperature is decreasing. In principle, the PLR can be reduced by increasing the primary flow rate and by this, an increased internal collector temperature would result in a lower efficiency. The maximum production is limited by the weather conditions as well as the minimum primary return temperature. The minimum production is a result from the technical maximum internal collector temperature. Further quantitative information is given in Table B1.

5.2. Case 2: Results for geothermal heating

Table 3 presents the correlation of the geothermal flow rate and the extraction temperature. Low flow rates result in lower supply temperatures through the increasing influence of the heat losses in the well on the geothermal medium due to the longer dwell time.

The results for the average variable costs of the geothermal heating plant are depicted in Fig. 4. In general, the costs are higher than for the solar thermal plant. This is induced particularly by the high electricity demand and the high electricity price for the downhole pump and additionally due to wear of parts and components. At full load, the requested temperature has only a small impact because of the high extraction temperature at high flow rates. But with decreasing PLR, the costs increase. This is particularly the case at a high temperature and low PLR. This effect is caused by the temperature to flow rate correlation. If the PLR is low and high temperatures are required, the flow rate must be high to generate the temperature. But due to the requested operational point, not all the energy is transferred inside the heat exchanger and thus the injection temperature increases. The unused exergy is reinjected into the ground. The maximum secondary temperature of 90 °C is limited to the maximum extraction temperature. The resulting data can be found in Table B2.

5.3. Case 3: Results for industrial surplus heating

The given conditions of the industrial processes result in the average variable costs shown in Fig. 5. As it can be seen, the costs are very low in general. An increase of the costs occurs at low temperature and full load. The high load requires a high flow rate if the resulting temperature difference between supply and return line is small. The high flow rate induces a higher electricity consumption.

Another interesting result is the maximum temperature related to the PLR. For a PLR below 33 % (100 kW), heat extraction is only possible from process B because the heat output of process A is not adjustable. At exactly 100 kW, process A can deliver its full thermal power and the maximum temperature of 95 °C. With an increasing PLR, an increasing amount of energy from process B is added. This results in a decrease of the maximum possible temperature for a higher PLR. The results are also presented in Table C1.

5.4. Comparison of presented heating plants

For the presented environmental conditions and assumptions, the solar thermal plant has only a small PLR control range. However, it can produce heat in a wide temperature range with the presented technology if the weather conditions are suitable. The result would be different for other weather conditions (is thus time-dependent). The small temperature impact is special for this specific type of vacuum tube collector and would be quite different for flat plate collectors [69].

The geothermal plant strongly depends on the conditions of the reservoir as well as on the electricity prices. In the presented case, the plant can control its PLR and supply temperature over the whole ranges except for temperatures above 90 °C. Lowering the PLR leads to higher

average variable costs. This effect is intensified at high temperatures.

The characteristics of the industrial surplus heating plant depend on the technology and the industrial site. This evaluation has shown that the PLR can be controlled in the complete range. However, high temperatures can only be achieved at smaller PLRs, which results in a trade-off between maximum PLR and maximum temperature.

For further graphical comparison, the data must be aggregated, which reduces the information but is helpful for the interpretation of the results. Fig. 6 has been created to demonstrate the utilization of the computed data. It shows the minimum average variable cost correlated to the PLR for all three case studies. The variable costs for the industrial surplus as well as for the solar-thermal heat are quite low and they seem to be acceptable over the full PLR range. As described above, the costs are rounded up to the minimum of 0.01 €/MWh and can therefore be even lower. For the given weather conditions, the solar thermal plant has a small range of PLR compared to the other plants. In the upper part of its PLR, a trade-off can be done between lower costs and slightly more production. The geothermal plant has quite high costs in general and with lower PLR the costs increase. The overall high costs of this plant can be explained by the high electricity prices in Germany as well as the non-optimal geological conditions which are assumed for this variant. Lower electricity costs would linearly reduce the costs for production in this case. Further, these results describe just the operative costs and they do not show the total variable costs which can behave quite different. However, these results allow for setting the plants' order in operation and emphasize the must-run condition for solar thermal and industrial surplus heating plants.

Fig. 7 shows the maximum supply temperature correlated to the PLR at the points of operation where the costs are lowest (as shown in Fig. 6). In other words, it shows the highest and most cost-effective temperature for each PLR. The dots show the original data at the discrete supply temperature pattern. The lines form the envelope curves. The solar thermal and the industrial surplus plant can supply their heat at their maximum temperature even though lowest costs are aimed. The limitations to the supply temperature are given by the technical restriction of these plants. The geothermal plant shows an increasing maximum supply temperature with an increasing PLR at lowest costs. This effect can be explained by the correlation of the extraction temperature to the flow rate in the geothermal reservoir. The higher the flow rate is, the less time does the geothermal medium take for the movement through the well and the lower is the temperature reduction through heat losses.

This comparison shows that temperature has a significant impact on the average variable costs and for different plant types, the correlation differs. In addition, their operation is not completely flexible (e.g. through weather conditions). Such plants that have low average variable costs like the presented solar thermal and industrial surplus heating plant would waste their energy if a requested PLR was too low or in some cases if a demanded supply temperature was too high. Therefore, it would be avoided in practice to reduce the PLR, even if it is possible to control the plant's thermal power beyond an optimal point of operation. Instead, from a systemic point of view, it is desirable to be able to combine different plants' operational points to create an overall optimum while considering their technical and conditional limitations.

The results can be used for qualitative discussions and to demonstrate the method, which is the objective of the paper. The case studies include the simplifications as well as parameters given in chapter 4 and therefore the quantitative results are site-specific. Particularly, those for the geothermal plant are sensitive to some specific inputs like the reservoir conditions as well as the electricity prices which are high in Germany. The complexity of this technology as well as the low public availability of data show that there is further demand for investigation. Nevertheless, the qualitative results are valid. For example, the geothermal plant will always have a non-optimal point of operation at low PLR and high temperature, even though the quantity of the impact can be much smaller or even higher. Sensitivity analyses for the used parameters could improve the accuracy for the quantitative results, to allow for more general statements of the magnitude of costs. For further improvements, the method could be extended with physical calculations that could consider the plant's dynamics (e.g. ramps between different points of operation) or non-constant return temperatures.

The presented case studies consider only a fraction of available heat generation technologies suitable for sustainable DHSs that can be evaluated with the proposed method. However, the resulting characteristics allow for some general conclusions. The suitability of the method is successfully demonstrated and an application to other heating sources and technologies (e.g. those with combustion processes) appears possible and desirable. The obtained results show the impact of supply temperature as well as PLR on the average variable costs and that the characteristics are very different for the different types of heat production plants. The results can also be used directly for the operational optimization of the given plants in Hamburg-Wilhelmsburg.

6. Conclusion

In modern district heating systems (DHSs), low supply temperatures are key to the integration of renewable heat sources. Therefore, current research is focused on innovative concepts that include controllable grid temperatures. To support these aspects adequately, the temperature impact on average variable heat production costs is evaluated in this paper.

The results of the paper are multiple. Firstly, a methodological gap in the current economical evaluation is identified which hinders a suitable choice of renewable heat sources as well as their integration in DHSs. It is shown that economic optimization and operational strategies do not sufficiently consider the dynamic control of supply temperature and part load ratio (PLR) of the heating plants yet. A method to properly address this integration is proposed and validated through the application to three case studies. The developed method allows for calculating and visualizing the average variable costs of heat production while considering supply temperature and PLR. By this means, it contributes as one part to fill the identified methodological gap and can provide cost transparency.

The method can be applied to all types of heat sources and technologies and is thus suitable to establish comparable databases. These data sets can be complemented by measurements of existing plants, particularly as measurement data will be increasingly available through the ongoing digitalization process in DHSs. Additionally, the method improves the informational basis for plant and grid design which should include the possibility to dynamically control the supply temperature and PLR. A subsequent step could be to apply the presented method to other parts of the DHS (e.g. storages, pipes, and buildings) to provide more transparency concerning the correlation of average variable costs to a chosen supply temperature.

In the presented cases, internal costs occurring from emissions do not play an important role, because emissions would only emerge from electricity generation and would be included in the electricity price. Including costs for emissions will become more relevant if renewable heat sources are compared to fossil ones. Furthermore, the presented method can also be adapted to compute average variable emissions that come from operation in correlation to supply temperature and PLR.

For investment and design decisions, the presented concept can support traditional calculations. It can be combined with the evaluation of costs for thermal power including capital (sunk) costs as well as fixed operational costs. This allows for an evaluation of levelized costs of heat. Only a full cost assessment can serve as a base to identify an ideal heating plant mix for each DHS.

Moreover, the results show that operational strategies should become more dynamic in order to provide the maximum energy efficiency at minimum costs. This applies in particular to DHSs that integrate many different types of renewable heat sources. The evaluation results should be included in further developments of optimization and control strategies that take advantage of dynamic supply temperatures. A more transparent and comprehensive methodology can be developed by combining the optimization of variable production costs as well as transportation costs (i.e. grid heat losses as well as electricity for the grid and energy central pumps). In such a methodology, also the costs should be considered that occur through lifetime reduction (wear) of the pipes. Further, a maximum number of temperature changes as well as gradient maxima could be introduced as a helpful boundary condition.

Indeed, the non-linearity and complexity of the resulting problem will be a challenge for traditional optimization concepts. A solution could be a numerical or data driven concept. An advantage of such approaches is that they are applicable to numerical models that are based on calculations, measurements, or state estimation. Results of the presented evaluation method could be used as discrete inputs for an optimization algorithm (e.g. linear solver or genetic algorithm).

A smart market would be an alternative approach. The smart market would require the variable costs as bids to provide a supply temperature at a given price. Under consideration of transportation costs and while meeting the heat demand, the smart market could determine an optimal (cheapest) combination of bids.

Just as the presented method for evaluating the correlation of average variable costs, supply temperature and PLR contributes to the creation of cost transparency, a smart market can also contribute to transparency beyond this by considering all costs. This could be supported by further development of the economic framework. After all, innovative pricing for heat could consider the demanded supply temperature, thus accelerating the DHS transformation process and enabling innovation and new business models.

Funding sources

This work was supported by the Federal Ministry for Economic Affairs and Energy of Germany in the project “Smart Heat Grid Hamburg” [grant number 03ET1458A].

CRediT authorship contribution statement

Peter Lorenzen: Conceptualization, Methodology, Software, Formal analysis, Investigation, Data curation, Writing – original draft, Writing – review & editing, Visualization, Project administration, Funding acquisition. **Carlos Alvarez-Bel:** Writing – review & editing, Supervision.

Declaration of Competing Interest

The authors declare that they have no known competing financial interests or personal relationships that could have appeared to influence the work reported in this paper.

Acknowledgment

We thank our colleagues for the great discussions and providing language help. We also thank our project partners from Hamburg Energie GmbH and eNeG GmbH who provide great expertise.

Appendix A. Input parameters for case studies

See Tables A1-A4.

Table A1
Solar thermal plant parameters.

Quantity	Value	Reference
Quadratic collector pressure coefficient	1,500,000 Pa · (l/s) $^{-1}$	[54]; pressure drop at 2 l/min is 13 mbar (XL 34P) and 19 mbar (XL 50P) resulting in a mean pressure drop of 16.6 mbar for both types. Coefficients are determined by quadratic regression.
Quadratic heat exchanger pressure coefficient	1000 Pa · (l/s) $^{-1}$	[70]; rough calculation had shown: Type AQ4 offers the required temperature gradient with acceptable pressure losses for the given maximal flow rate. Pressure loss coefficients are determined by quadratic regression from maximum pressure at maximum flow rate.
Length of collector connecting pipes (series)	14.4 m	Estimated by building dimensions.
Inner diameter of collector connecting pipes (series)	22.9 mm	Calculated by rough design study based in maximum operation.
Length of main pipes	156 m	Estimated by building dimensions.
Inner diameter of main pipes	83.4 mm	Calculated by rough design study based in maximum operation.
Pipe surface roughness	0.05 mm	[42]; steel, good finish.
Nominal pump efficiency	0.72	[71]; Pump “Grundfoss TPE 50–290/2” selected by maximum flow rate and pressure difference.

Table A2
Technical geothermal plant parameters.

Quantity	Value	Reference
Density of geothermal medium	1147 kg/m^3	[58]; assumed to be constant; depends on water chemistry and temperature.
Heat capacity of geothermal medium	3,5 kJ/(kg K)	[58]; assumed to be constant; depends on water chemistry and temperature.
Wellhead pressure	10 bar	[58]; defined by geochemistry.
Nominal pump efficiency (at 70 l/s)	0.75	[58]; given by pump characteristics.
Static fluid layer height	100 m	Depending on geological characteristics; estimated; plausibility checked by comparing results with [58].
Well diameter	155 mm	Assumption related to [60]; would be chosen by constructors.
Well surface roughness	0.013 mm	Estimated based on [60].
Min. (rel.) thermal power	0.1	Assumption to typical pump characteristics.
Geothermal productivity index	30 m^3/h/MPa	[58]; depending on geological characteristics.
Thermal conductivity	4 W/m/K	[61]; typical value for liquid dominated well.

Table A3
Economical geothermal plant parameters.

Quantity	Value	Reference
Subsurface investment for a 3000 m well doublet including all costs	14,850,000 €	cf. [58]
Surface investment for heating plant including all costs	1,199,000 €	cf. [58]
Share of maintenance on subsurface investment	1.5 %	[58]
Share of maintenance on surface investment	6 %	[58]
Planned annual runtime	7500 h/a	[58]

Table A4
Industrial surplus heating plant parameters.

Quantity	Value	Reference
Distance of industry to DHS	300 m	[68]
Nominal pump efficiency	0.7	Assumption based on typical values.
Quadratic pressure coefficient for heat exchanger	1000 Pa · (l/s)$^{-1}$	[70]; rough calculation had shown: type AQ4 offers the needed temperature gradient with acceptable pressure losses for the given maximal flow rate. Pressure loss coefficients are determined by quadratic regression from maximum pressure at maximum flow rate.
Secondary supply temperature of the chilling process	75 °C	[72]; assumption related to reference.
Secondary supply temperature of the exhaust gas process	95 °C	[72]; higher temperatures from exhaust gas are possible. For cheaper system design, temperatures below 100 °C are assumed.
Pipe surface roughness	0.05 mm	[42]; steel, good finish.

Appendix B. Quantitative results of the case studies

See Tables B1-B3.

Table B1
Average variable costs in €/MWh of the solar thermal plant at 700 W/m^2 and 18 °C correlated to supply temperature (rows) and part load ratio (columns).

T_s \ PLR	60.0 %	62.5 %	65.0 %	67.5 %	70.0 %	72.5 %	73.0 %	73.5 %	74.0 %
60.0 °C	0.647	0.057	0.015	0.006	0.009	0.041	0.061	0.102	0.193
72.5 °C	0.647	0.057	0.015	0.006	0.009	0.041	0.061	0.102	0.193
77.5 °C	0.647	0.057	0.015	0.006	0.009	0.041	0.061	0.101	0.193
80.0 °C	0.647	0.057	0.015	0.006	0.009	0.041	0.061	0.103	
82.5 °C	0.647	0.057	0.015	0.006	0.009	0.041	0.061	0.103	
85.0 °C	0.647	0.057	0.015	0.006	0.009	0.041	0.061		
87.5 °C	0.647	0.057	0.015	0.006	0.009	0.041	0.061		
90.0 °C	0.647	0.057	0.015	0.006	0.009	0.041			
95.0 °C	0.647	0.057	0.015	0.006	0.009	0.041			

Table B2
Average variable costs in €/MWh of the geothermal plant correlated to supply temperature (rows) and part load ratio (columns).

T_s \ PLR	10.0 %	20.0 %	30.0 %	40.0 %	50.0 %	60.0 %	70.0 %	80.0 %	90.0 %	100.0 %
60.0 °C	54	32	25	23	22	22	22	22	23	24
75.0 °C	54	32	25	23	22	22	22	22	23	24
77.5 °C	57	32	25	23	22	22	22	22	23	24
80.0 °C	60	32	25	23	22	22	22	22	23	24
82.5 °C	66	33	25	23	22	22	22	22	23	24
85.0 °C	80	40	27	23	22	22	22	22	23	24
87.5 °C	114	57	38	28	23	22	22	22	23	24
90.0 °C	240	120	80	60	48	40	34	30	27	24

Table B3
Average variable costs in €/MWh of the industrial surplus heat plant correlated to supply temperature (rows) and part load ratio (columns).

T_s \ PLR	10.0 %	20.0 %	30.0 %	40.0 %	50.0 %	60.0 %	70.0 %	80.0 %	90.0 %	100.0 %
60.0 °C	0.006	0.025	0.055	0.096	0.148	0.211	0.285	0.371	0.467	0.573
62.5 °C	0.003	0.013	0.028	0.050	0.077	0.109	0.148	0.192	0.242	0.297
65.0 °C	0.002	0.008	0.017	0.029	0.045	0.064	0.086	0.112	0.141	0.174
67.5 °C	0.001	0.005	0.011	0.018	0.029	0.041	0.055	0.071	0.090	0.110
70.0 °C	0.001	0.003	0.007	0.012	0.019	0.027	0.037	0.048	0.061	0.074
72.5 °C	0.001	0.002	0.005	0.009	0.014	0.019	0.026	0.034	0.043	0.053
75.0 °C	0.001	0.002	0.004	0.006	0.01	0.014	0.019	0.025	0.031	0.039
77.5 °C				0.005	0.008	0.011	0.015	0.019	0.024	0.029
80.0 °C				0.004	0.006	0.008	0.011	0.015		
82.5 °C				0.003	0.005	0.007				
85.0 °C				0.002	0.004					
87.5 °C				0.002						

References

[1] UNFCCC. The Paris Agreement. In: Paris Climate Change Conference - November 2015; 2015. https://unfccc.int/process-and-meetings/the-paris-agreement/the-paris-agreement.

[2] IEA. Renewables 2020, Paris; 2020. https://www.iea.org/reports/renewables-2020.

[3] United Nations Environment Programme. District Energy in Cities: Unlocking the Potential of Energy Efficiency and Renewable Energy; 2015. https://www.unep.org/resources/report/district-energy-cities-unlocking-potential-energy-efficiency-and-renewable-energy.

[4] Lund H, Werner S, Wiltshire R, Svendsen S, Thorsen JE, Hvelplund F, et al. 4th Generation District Heating (4GDH): Integrating smart thermal grids into future sustainable energy systems. Energy 2014;68:1–11. https://doi.org/10.1016/j.energy.2014.02.089.

[5] Volkova A, Mašatin V, Siirde A. Methodology for evaluating the transition process dynamics towards 4th generation district heating networks. Energy 2018;150:253–61. https://doi.org/10.1016/j.energy.2018.02.123.

[6] Averfalk H, Werner S. Economic benefits of fourth generation district heating. Energy 2020;193:116727. https://doi.org/10.1016/j.energy.2019.116727.

[7] Lund R, Østergaard DS, Yang X, Mathiesen BV. Comparison of Low-temperature District Heating Concepts in a Long-Term Energy System Perspective. Int J Sustain Energy Planning Manage 2017;12. https://doi.org/10.5278/IJSEPM.2017.12.2.

[8] Lund H, Duic N, Østergaard PA, Mathiesen BV. Future district heating systems and technologies: On the role of smart energy systems and 4th generation district heating. Energy 2018;165:614–9. https://doi.org/10.1016/j.energy.2018.09.115.

[9] Nord N, Nielsen EKL, Kauko H, Tereshchenko T. Challenges and potentials for low-temperature district heating implementation in Norway. Energy 2018;151:889–902. https://doi.org/10.1016/j.energy.2018.03.094.

[10] Frederiksen S, Werner S. District Heating and Cooling. Studentlitteratur AB; 2013, ISBN 978-91-44-08530-2.

[11] Buffa S, Cozzini M, D'Antoni M, Baratieri M, Fedrizzi R. 5th generation district heating and cooling systems: A review of existing cases in Europe. Renew Sustain Energy Rev 2019;104:504–22. https://doi.org/10.1016/j.rser.2018.12.059.

[12] Abugabbara M, Javed S, Bagge H, Johansson D. Bibliographic analysis of the recent advancements in modeling and co-simulating the fifth-generation district heating and cooling systems. Energy Build 2020;224:110260. https://doi.org/10.1016/j.enbuild.2020.110260.

[13] Rämä M, Wahlroos M. Introduction of new decentralised renewable heat supply in an existing district heating system. Energy 2018;154:68–79. https://doi.org/10.1016/j.energy.2018.03.105.

[14] Moallemi A, Arabkoohsar A, Pujatti FJP, Valle RM, Ismail KAR. Non-uniform temperature district heating system with decentralized heat storage units, a reliable solution for heat supply. Energy 2019;167:80–91. https://doi.org/10.1016/j.energy.2018.10.188.

[15] Arabkoohsar A. Non-uniform temperature district heating system with decentralized heat pumps and standalone storage tanks. Energy 2019;170:931–41. https://doi.org/10.1016/j.energy.2018.12.209.

[16] Kim J, Weidlich I. Identification of Individual District Heating Network Conditions using Equivalent Full Load Cycles. Energy Proc 2017;116:343–50. https://doi.org/10.1016/j.egypro.2017.05.081.

[17] Schmidt D, Kallert A, Blesl M, Svendsen S, Li H, Nord N, et al. Low Temperature District Heating for Future Energy Systems. Energy Proc 2017;116:26–38. https://doi.org/10.1016/j.egypro.2017.05.052.

[18] Olsthoorn D, Haghighat F, Mirzaei PA. Integration of storage and renewable energy into district heating systems: A review of modelling and optimization. Sol Energy 2016;136:49–64. https://doi.org/10.1016/j.solener.2016.06.054.

[19] Enrico S, Wall G. A brief Commented History of Exergy From the Beginnings to 2004. Int J Thermodyn 2007;10:3. https://doi.org/10.5541/ijot.184.

[20] Lazzaretto A, Tsatsaronis G. SPECO: A systematic and general methodology for calculating efficiencies and costs in thermal systems. Energy 2006;31:1257–89. https://doi.org/10.1016/j.energy.2005.03.011.

[21] Alkan MA, Keçebaş A, Yamankaradeniz N. Exergoeconomic analysis of a district heating system for geothermal energy using specific exergy cost method. Energy 2013;60:426–34. https://doi.org/10.1016/j.energy.2013.08.017.

[22] Di Somma M, Yan B, Bianco N, Graditi G, Luh PB, Mongibello L, et al. Multi-objective design optimization of distributed energy systems through cost and exergy assessments. Appl Energy 2017;204:1299–316. https://doi.org/10.1016/j.apenergy.2017.03.105.

[23] Pirouti M, Bagdanavicius A, Ekanayake J, Wu J, Jenkins N. Energy consumption and economic analyses of a district heating network. Energy 2013;57:149–59. https://doi.org/10.1016/j.energy.2013.01.065.

[24] Vesterlund M, Toffolo A, Dahl J. Optimization of multi-source complex district heating network, a case study. Energy 2017;126:53–63. https://doi.org/10.1016/j.energy.2017.03.018.

[25] Bavière R, Vallée M. Optimal Temperature Control of Large Scale District Heating Networks. Energy Proc 2018;149:69–78. https://doi.org/10.1016/j.egypro.2018.08.170.

[26] Fang T, Lahdelma R. Genetic optimization of multi-plant heat production in district heating networks. Appl Energy 2015;159:610–9. https://doi.org/10.1016/j.apenergy.2015.09.027.

[27] Raffensperger JF, Milke MW. Smart Markets for Water Resources: A Manual for Implementation. Cham: Springer International Publishing; 2017, ISBN 978-3-319-55008-4.

[28] Sorknæs P, Lund H, Skov IR, Djørup S, Skytte K, Morthorst PE, et al. Smart Energy Markets - Future electricity, gas and heating markets. Renew Sustain Energy Rev 2020;119:109655. https://doi.org/10.1016/j.rser.2019.109655.

[29] McCabe KA, Rassenti SJ, Smith VL. Smart Computer-Assisted Markets. Science 1991;254:534–8. https://doi.org/10.1126/science.254.5031.534.

[30] McCabe KA, Rassenti SJ, Smith VL. Designing 'smart' computer-assisted markets: An experimental auction for gas networks. Eur J Polit Econ 1989;5:259–83. https://doi.org/10.1016/0176-2680(89)90049-9.

[31] Li C-F, Li J-S. Fair allocation using a fast smart market auction. Eur J Oper Res 2006;172:352–65. https://doi.org/10.1016/j.ejor.2004.10.006.

[32] Murphy JJ, Dinar A, Howitt RE, Rassenti SJ, Smith VL, Weinberg M. The design of water markets when instream flows have value. J Environ Manage 2009;90:1089–96. https://doi.org/10.1016/j.jenvman.2008.04.001.

[33] Lorenzen P. A District Heating Market Mechanism – Markets as a Mature Concept for a Modern District Heating Infrastructure. Hot|Cool 2019;3(2019):22–4. http://www.e-pages.dk/dbdh/71/.

[34] Quaschning V. Regenerative Energiesysteme - Technologie - Berechnung - Simulation. 2nd ed. München: Hanser; 2015, ISBN 978-3-446-44267-2. p. 122–4.

[35] Zelewski S. Petrinetzbasierte Modellierung komplexer Produktionssysteme: Band 2: Bezugsrahmen, vol. 6, Leipzig: Universität Leipzig, Institut für Produktionswirtschaft und industrielle Informationswirtschaft; 1995.

[36] Harris CR, Millman KJ, van der Walt SJ, Gommers R, Virtanen P, Cournapeau D, et al. Array programming with NumPy. Nature 2020;585:357–62. https://doi.org/10.1038/s41586-020-2649-2.

[37] The Pandas Development Team, pandas-dev/pandas: Pandas, Zenodo; 2020. https://doi.org/10.5281/zenodo.3509134.

[38] McKinney W. Data Structures for Statistical Computing in Python 2010:56–61. https://doi.org/10.25080/Majora-92bf1922-00a.

[39] Østergaard DS, Svendsen S. Costs and benefits of preparing existing Danish buildings for low-temperature district heating. Energy 2019;176:718–27. https://doi.org/10.1016/j.energy.2019.03.186.

[40] Hunter JD. Matplotlib: A 2D graphics environment. Comput Sci Eng 2007;9:90–5. https://doi.org/10.1109/MCSE.2007.55.

[41] Lorenzen P, Janßen P, Winkel M, Klose D, Kernstock P, Schrage J, et al. Design of a Smart Thermal Grid in the Wilhelmsburg district of Hamburg: Challenges and approaches. Energy Proc 2018;149:499–508. https://doi.org/10.1016/j.egypro.2018.08.214.

[42] Müller MR. Simulationsmodell für vermaschte Rohrnetze. Hamburg 2017. https://reposit.haw-hamburg.de/handle/20.500.12738/8309.

[43] Wagner W. Strömung und Druckverlust: mit Beispielsammlung. 6., bearb. Aufl. ed. Würzburg: Vogel; 2008, ISBN 978-3-8343-3132-8.

[44] Born R, Brüchler F. Grundlagen für die Planung von Kreiselpumpenanlagen, 7th ed. Sterling SIHI GmbH; 2000. p. 38, 61-62.

[45] Kind M, Martin H. VDI-Wärmeatlas, 11th ed., Berlin, Heidelberg: Springer Berlin Heidelberg; 2013, pp. 176-177. https://doi.org/10.1007/978-3-642-19981-3_1.

[46] "Stromsteuer," Generalzolldirektion, 10 2 2020. [Online]. Available: https://www.zoll.de/DE/Fachthemen/Steuern/Verbrauchsteuern/Strom/strom_node.html.

[47] Bundesnetzagentur, "Preise und Rechnungen," 10/02/2020. [Online]. Available: https://www.bundesnetzagentur.de/DE/Sachgebiete/ElektrizitaetundGas/Verbraucher/PreiseRechnTarife/preiseundRechnungen-node.html.

[48] 50Hertz Transmission GmbH, Amprion GmbH, TransnetBW GmbH, "Informationsplattform der deutschen Übertragungsnetzbetreiber," 10/02/2020. [Online]. Available: https://www.netztransparenz.de.

[49] Bundesministerium der Justiz und für Verbraucherschutz, "Konzessionsabgabenverordnung (KAV) – § 2 Bemessung und zulässige Höhe der Konzessionsabgaben," 10/02/2020. [Online]. Available: http://www.gesetze-im-internet.de/kav/_2.html.

[50] Stromnetz Hamburg, "Preisblatt Netzentgelte,"; 2020. [Online]. Available: https://www.stromnetz-hamburg.de/download/netzentgelte-2020/?wpdmdl=17113.

[51] Fraunhofer ISE, "Jährliche Börsenstrompreise in Deutschland," 12/08/2020. [Online]. Available: https://www.energy-charts.de/price_avg_de.htm?price=nominal&period=annual&year=2019.

[52] Ritter XL. Energiebunker Wilhelmsburg: Ehemaliger Flakbunker gewinnt Sonnenwärme für Hamburger Fernwärmenetz. [Online] Available: https://www.ritter-xl-solar.de/anwendungen/waermenetze/energiebunker-wilhemsburg/.

[53] ITW University Stuttgart. Annex to Solar Keymark Certificate - AQUA PLASMA. 15/04/2020. [Online]. Available: http://www.solarkeymark.nl/DBF/PDF_Downloads/DS_355.pdf.

[54] Paradigma. Solarwärme-Systeme. 15/04/2020. [Online]. Available: http://www.koop-vondoehlen.de/Bilder/pdf/Paradigma/kollektor.pdf.

[55] DIN EN 12975-1: Thermal solar systems and components - Solar collectors - Part 1: General requirements; 2011.

[56] Reda F. Solar Assisted Ground Source Heat Pump Solutions: Effective Energy Flows Climate Management. Cham: Springer International Publishing; 2017. p. 14. https://doi.org/10.1007/978-3-319-49698-6_2.

[57] Hamburg Energie Geothermie. FAQ / Häufig gestellte Fragen: Wie tief wird gebohrt?; 2021. https://www.geothermie-wilhelmsburg.de/faq/.

[58] Huenges E. Geothermal Energy Systems - Exploration, Development, and Utilization. 2nd ed. Weinheim: WILEY-VCH Verlag; 2012, ISBN 978-3-527-40831-3.

[59] Agemar T, Weber J, Schulz R. Deep Geothermal Energy Production in Germany. Energies 2014;7:4397–416. https://doi.org/10.3390/en7074397.

[60] Stober I, Bucher K. Geothermie 2014:220. ISBN 978-3-642-41763-4, pp. 35, 150.

[61] Aydin H, Merey S. Design of Electrical Submersible Pump system in geothermal wells: A case study from West Anatolia, Turkey. Energy 2021;230:120891. https://doi.org/10.1016/j.energy.2021.120891.
[62] Kullick J, Hackl CM. Dynamic Modeling and Simulation of Deep Geothermal Electric Submersible Pumping Systems. Energies 2017;10. https://doi.org/10.3390/en10101659.
[63] Aydin H, Akin S, Senturk E, Tuzen MK. Artificial Lifting in Liquid Dominated High Temperature Geothermal Fields in Turkey: Lessons Learned. In: 46th Workshop on Geothermal Reservoir Engineering, Stanford University, 2021. https://pangea.stanford.edu/ERE/pdf/IGAstandard/SGW/2021/Aydin2.pdf.
[64] Blöcher G, Reinsch T, Henninges J, Milsch H, Regenspurg S, Kummerow J, et al. Hydraulic history and current state of the deep geothermal reservoir Groß Schönebeck. Geothermics 2016;63:27–43. https://doi.org/10.1016/j.geothermics.2015.07.008.
[65] Zimmermann J, Budach I, Metz M, Barth G, Franz M, Seibt P, et al. Reservoir prediction and risk assessment of hydrothermal reservoirs in the North German Basin – combining deep subsurface reservoir mapping with Monte-Carlo Simulation. In: Proceedings European Geothermal Congress 2019, Den Haag, 06/2019; 2019. https://europeangeothermalcongress.eu/wp-content/uploads/2019/07/221.pdf.
[66] Moser S, Puschnigg S, Rodin V. Designing the Heat Merit Order to determine the value of industrial waste heat for district heating systems. Energy 2020;200:117579. https://doi.org/10.1016/j.energy.2020.117579.
[67] Papapetrou M, Kosmadakis G, Cipollina A, Commare UL, Micale G. Industrial waste heat: Estimation of the technically available resource in the EU per industrial sector, temperature level and country. Appl Therm Eng 2018;138:207–16. https://doi.org/10.1016/j.applthermaleng.2018.04.043.
[68] Wessel K, Maaß S, Reckschwardt R. Inernationale Bauaustellung Hamburg – Energiebunker. 01/04/2014. [Online]. Available: https://epub.sub.uni-hamburg.de//epub/volltexte/2015/40526/pdf/140610_WHI_EB_final.pdf.
[69] Rosa AD, Boulter R, Church K, Svendsen S. District heating (DH) network design and operation toward a system-wide methodology for optimizing renewable energy solutions (SMORES) in Canada: A case study. Energy 2012;45:960–74. https://doi.org/10.1016/j.energy.2012.06.062.
[70] Alfa Laval. Heiz- und Kühllösungen von Alfa Laval. 2013. [Online]. Available: http://www.aptec.at/uploads/Upload-Container-Downloads/Alfa Laval Produktkatalog.pdf.
[71] Grundfoss. Product Selection Center. 12/08/2020. [Online]. Available: https://product-selection.grundfos.com/front-page.html.
[72] Grahl A, Joest S, Raulien T. Erfolgreiche Abwärmenutzung im Unternehmen – Energieeffizienzpotenziale erkennen und erschließen. 01/12/2015. [Online]. Available: https://www.dena.de/fileadmin/dena/Publikationen/PDFs/2019/1445_Broschuere_Abwaermenutzung.pdf.